

Observation of the Wave Function of a Quantum Billiard from the Transverse Patterns of Vertical Cavity Surface Emitting Lasers

K. F. Huang, Y. F. Chen,* and H. C. Lai

Department of Electrophysics, National Chiao Tung University, Hsinchu, Taiwan, Republic of China

Y. P. Lan

Institute of Electro-Optical Engineering, National Chiao Tung University, Hsinchu, Taiwan, Republic of China

(Received 26 April 2002; published 11 November 2002)

We demonstrate experimentally that the near-field and far-field transverse patterns of a large aperture vertical cavity surface emitting laser (VCSEL) can be successfully interpreted as a two-dimensional (2D) billiard system. It is found that the near-field and far-field transverse patterns of a large aperture VCSEL evidently represent the coordinate-space and momentum-space wave functions of a 2D quantum billiard, respectively. The result of this paper suggests that large aperture VCSELs are potentially appropriate physical systems for the wave-function study in quantum problems.

DOI: 10.1103/PhysRevLett.89.224102

PACS numbers: 05.45.Mt, 42.55.Sa, 42.60.Jf

Vertical cavity surface emitting lasers (VCSELs) have become of considerable interest for short-range data communications and sensor applications [1]. Of scientific interest, VCSELs inherently emit in single-longitudinal mode due to their extremely short cavity length, but large aperture devices can exhibit a complex transverse mode structure. The transverse mode pattern and the polarization instabilities in VCSELs have been the main interests in the past few years [2–7]. Hegarty *et al.* [8] reported interesting transverse mode patterns from oxide-confined square-shaped VCSELs with larger aperture. Their experimental results revealed that a wave incident upon the current-guiding oxide boundary would undergo total internal reflection because of large index discontinuities between the oxide layer and the surrounding semiconductor material. Namely, VCSELs can be considered as a planar waveguide with a dominant wave vector along the vertical direction. Because of the analogy between the Schrodinger and Helmholtz equations [9], it is essentially feasible to use the oxide-confined VCSEL cavities, such as microwave cavities [10,11], to represent quantum mechanical potential wells. In this case, the transverse patterns can reveal the probability density of the corresponding wave functions to the two-dimensional quantum billiards. However, such a correspondence has not been established as yet because the thermal effects usually result in a complex refraction-index distribution to distort the VCSEL planoplanar resonators [6].

In this Letter, we experimentally demonstrate that, when the thermal effects are reduced by cooling the device at the temperature below 10 °C, the near-field and far-field transverse patterns of a large aperture VCSEL evidently represent the coordinate-space and momentum-space wave functions of a 2D quantum billiard, respectively. The satisfactory correspondence implies that VCSELs are appropriate devices for the study of the behavior of the wave functions in quantum billiard prob-

lems. Since VCSELs, in general, can be fabricated for any two-dimensional shape, this versatility makes these devices extremely flexible to explore a great deal of interesting physics.

In this investigation, we fabricate square-shaped VCSELs with large aperture and measure near-field and far-field patterns of the transverse mode. The size of the oxide aperture is $40 \times 40 \mu\text{m}^2$. The device structure of these oxide-confined VCSELs and the methods used to measure the far-field and near-field patterns are similar to those described by Ref. [8]. Experimental results show that the transverse patterns of VCSELs can be certainly divided into two regimes of low-divergence and high-divergence emissions. Hereafter, we will concentrate on the high-divergence emission, which appears only at reduced temperature and near threshold operation. It is expected the thermal-lensing effect will switch the device into the low-divergence regime because the joule heating induces a temperature rise across the device cross section. Typically, high-divergence patterns are very symmetric and those of low divergence are more irregular. Therefore it is easy to differentiate the regimes in which the lasers are being operated.

We first controlled the device at the temperature of 10 °C. As shown in Fig. 1, the near-field pattern of the device was found to be a bouncing-ball scar that is similar to the result of Ref. [8], except that the order is higher. It can be seen that the observed bouncing-ball scar is not perfectly periodic but contains dislocations to show some wavy structure. Even so, the laser beam was measured to be linearly polarized. As the device was cooled at the temperature around 0 °C, the near-field pattern changed dramatically, as shown in Fig. 2. It can be seen that the near-field intensity apparently was highly concentrated along the trajectory of a diamond-shaped classical orbit. Although this diamond “scar” has been discussed extensively in the wave functions of ballistic quantum dots

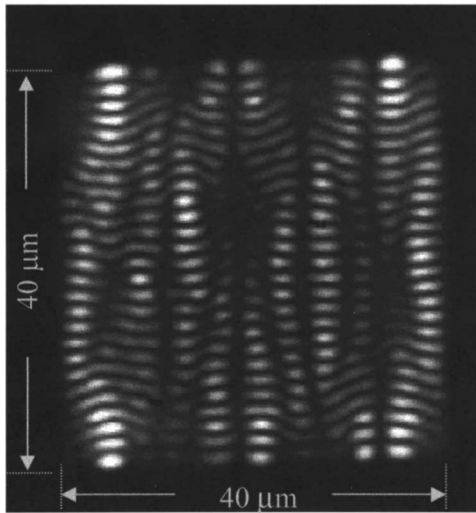


FIG. 1. The experimental result for the near-field pattern of the VCSEL device near the lasing threshold. The device was operated at the temperature 10 °C.

[12–14], it is the first time to observe this interesting pattern from a laser transverse pattern. The specific wave scars confirm the fact that the oxide-confined VCSELs can be considered as a planar waveguide.

In order to understand the observed transverse patterns, it is helpful to simplify the VCSEL structure first. We consider the large aperture VCSEL to be a very narrow square-shaped three-dimensional resonator with embedded gain material. The two distributed feedback reflectors (DBR) were separated by nearly one wavelength and the square-shaped oxide aperture defined the lateral billiard boundary. The wave vectors can be decomposed into k_z and k_t , where k_z is the wave-vector component along the direction of vertical emission and k_t is the transverse wave-vector component. Since the vertical dimension is designed to be nearly one wavelength, k_z is the dominating component in the emission wave vector. The lateral boundary has a dimension of $40 \times 40 \mu\text{m}^2$; consequently, the transverse k_t is much smaller than k_z . The lateral oxide boundary can be considered as rigid walls with infinite potentials since the photons will experience total reflection at the lateral oxide walls due to a large k_z component and a relatively small transverse component k_t . Furthermore, since the mirrors in VCSELs are DBRs, they can be considered as plane mirrors with no curvature. The photons can be treated as particles confined in a boundary with infinite potential and zero potential inside the square. Vertical emission in the z direction can be considered to be the coupling of the resonance fields inside the cavity to the outside medium through the top DBR. Therefore, the phasor amplitude of the emission field distribution $E(x, y, z)$ is conveniently given by $E(x, y, z) = \psi(x, y)e^{-jk_z z}$. After separating the z component in the wave equation, we are left with a two-dimensional Helmholtz equation: $(\nabla_t^2 + k_t^2)\psi(x, y) = 0$. Here, ∇_t^2 means the Laplacian operator operating on the

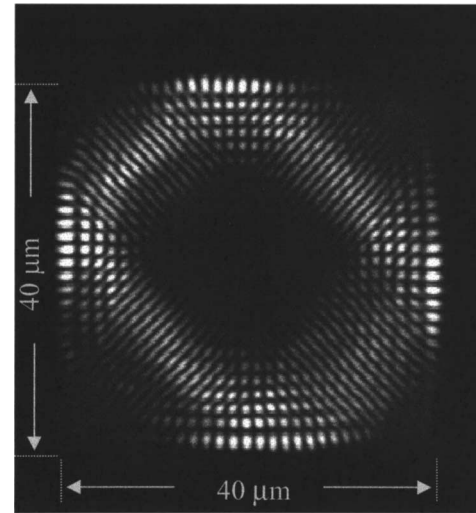


FIG. 2. The experimental result for the near-field pattern of the VCSEL device near the lasing threshold. The device was operated at the temperature 0 °C.

coordinates in the transverse plane and $\psi(x, y)$ is a scalar wave function that describes the transverse profile of the laser. The solutions to the Helmholtz equation with total internal reflection boundaries are equivalent to the solutions of the 2D Schrodinger equation with hard wall boundaries [$\psi(x, y) = 0$ at the boundary] of the same geometry. This analogy has been exploited most successfully in microwave cavities and scarred eigenfunctions of a chaotic billiard have been demonstrated [10,11]. The wave functions for the 2D quantum billiards are also important understanding the behavior of mesoscopic structures, and will be crucial for the design of nanoscale electronic devices [12–14].

It is well known that the solution to a perfect square billiard can be obtained by separation of variables. However, this subtle solution definitely cannot account for the present observed pattern. It is self-evident that the perfect square billiard is quite rare in most of the real physical problems. In real VCSEL devices, the square aperture is fabricated first by etching a square mesa and then oxidizes the AlAs layer to form the oxide boundary. Process induced deformation is unavoidable, and therefore a perfect square billiard is not appropriate for the simulation. In order to simulate the square billiard formed by the oxide aperture, we modify the square by rounding off the corners. With the rounded off square boundary, the Helmholtz equation can no longer be solved by the method of separation of variables. We use a numerical method called expansion method [15] to solve the equation. Because of symmetry breaking, the eigenfunctions obtained are much more interesting than those of the perfect square billiard. For low order solutions, the patterns are similar to those of the perfect square billiard. However, the higher order eigenfunctions are drastically different in structure and very rich patterns appear. It is of surprising interest that some of the solutions display the

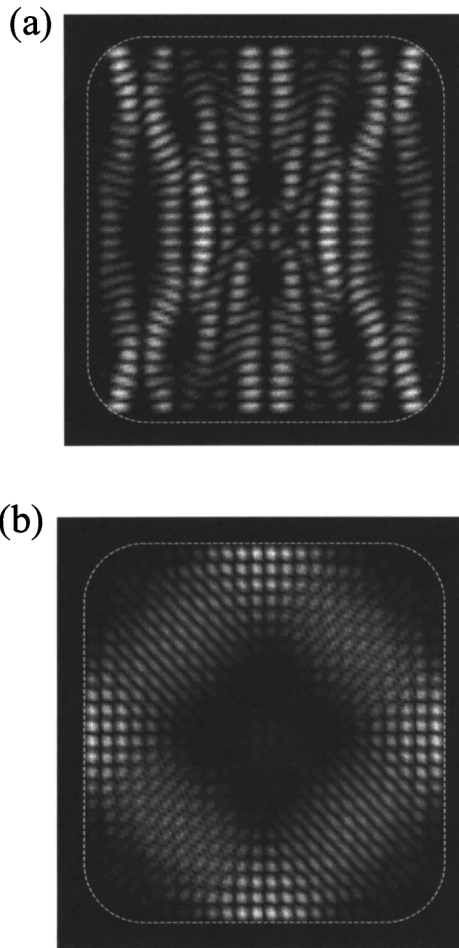


FIG. 3. The calculated wave functions of the square billiards modified by rounding off the corners. (a) and (b) are similar to the observed near-field patterns in Figs. 1 and 2, respectively. The dashed lines indicate the boundary of the simulation.

distorted bouncing-ball and diamond-shaped scars similar to the experimental results. Figure 3 shows two of the calculated eigenfunctions that are similar to the observed near-field patterns in Figs. 1 and 2. Note that the present modified square billiards always have the high-order eigenfunctions demonstrating the distorted bouncing-ball and diamond-shaped scars, almost irrelevant to the degree of how much the corners are rounded off.

It is worthwhile to mention that Nöckel and Stone [16] have designed stadium-shaped microcavity lasers and demonstrated high power directional emission in the midinfrared wavelength based on some chaotic two-dimensional billiard dynamics. However, due to the geometrical structure of the laser, only edge emission was allowed in these deformed microdisk lasers. Therefore, a comparison between the experimentally determined far-field pattern and simulation was limited for only one dimension. The near-field pattern was not measured because high-resolution midinfrared detection was not possible.

The optical far-field intensity essentially is the spatial 2D Fourier transform (FT) of the near-field pattern,

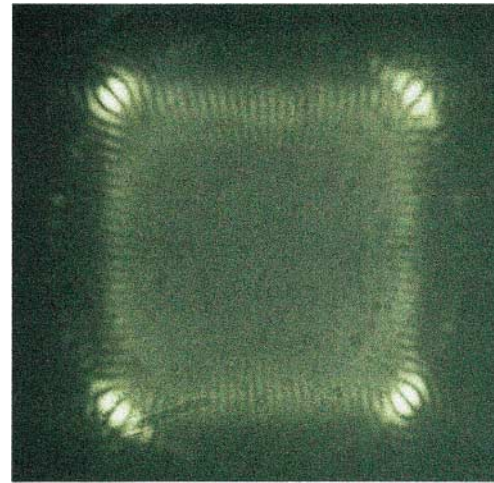


FIG. 4 (color). The experimental result for the far-field pattern corresponding to the near-field pattern in Fig. 2.

responds to the momentum-space representation in the quantum mechanics. Recently, Delande and Sornette [17] have calculated the acoustic radiation from a stadium-shaped membrane by applying FT to the eigenfunctions. Similar calculations focusing on the momentum representation of the wave functions were also reported by Bäcker and Schubert [18]. Both theoretical papers suggested that momentum distribution of a two-dimensional quantum billiard is actually experimentally observable and such information can provide a more comprehensive understanding to the billiard system. Therefore, it is consequentially meaningful to measure the far-field pattern for the VCSEL devices. Figure 4 shows the experimental observation of the far-field pattern corresponding to the diamond-shaped wave function in Fig. 2. It can be clearly seen that the far-field pattern exhibited some strong intensity lotus flower structure at the corners of the square and some weak stripes connecting the lotus structure. This far-field pattern is consistent with the near-field

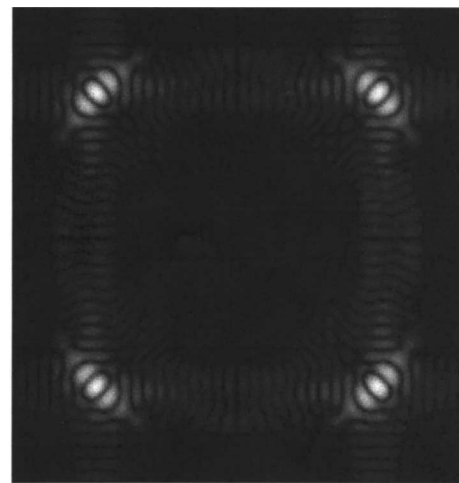


FIG. 5. The calculated momentum-space wave function corresponding to the coordinate-space wave function in Fig. 3(b).

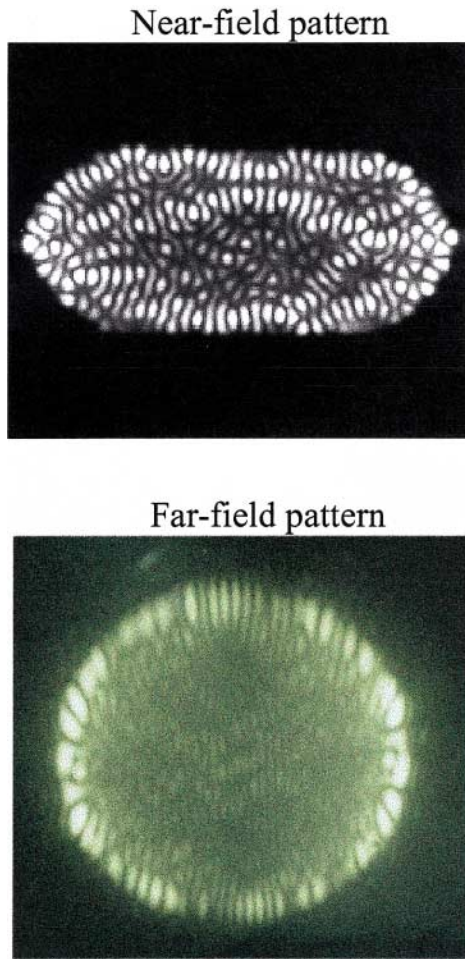


FIG. 6 (color). Experimental results of the near-field and far-field patterns for the VCSEL device with a stadium-shaped boundary.

diamond-shaped scar that apparently was concentrated along the trajectory traced by a particle bouncing off the neighboring walls of the square. Figure 5 shows the momentum-space wave function of the theoretical diamond-shaped scar shown in Fig. 3. The good agreement between experimental results and theoretical calculations confirms our physical analysis and validates the present theoretical model.

Finally, it is worthwhile to clarify that the present interpretation is based on the assumption that the influence of carrier dynamics on the transverse pattern near threshold is negligible. To further justify this assumption, we fabricated the devices with a shape of Bunimovich stadium boundary and measured the near-field and far-field intensities. As shown in Fig. 6, the near-field intensity displays a scarred pattern and the far-field intensity resembles the calculated results of Refs. [17,18] in appearance. The boundary-shape dependence of the VCSEL patterns confirms the present interpretation.

In conclusion, we have observed unique near- and far-field transverse patterns in large aperture VCSELs. A two-dimensional quantum billiard model is utilized to

explain the experiments. It turns out the square billiard with minor modification is adequate to simulate the real device. Rounding off the corners certainly breaks the symmetry and introduces coupling of the two originally independent variables. This symmetry breaking makes the solution of the high-order eigenfunctions much more interesting as they display highly graphical patterns. The observed near-field pattern in the transverse mode apparently can be interpreted as from these solutions. Furthermore, the corresponding far-field patterns can also be explained by the momentum-space wave functions in the billiard. The result of this paper also suggests that large aperture VCSELs are potentially appropriate physical systems for the quantum chaos study.

The authors gratefully acknowledge various VCSEL devices from TrueLight Corporation. The authors also thank the National Science Council for their financial support of this research under Contract No. NSC-91-2112-M-009-030.

*Corresponding author.

Electronic address: yfchen@cc.nctu.edu.tw

- [1] W.W. Chow, K. D. Choquette, M. Hagerot-Crowford, K. L. Lear, and G. R. Hadley, *IEEE J. Quantum Electron.* **33**, 1810 (1997).
- [2] M. San Miguel, Q. Feng, and J.V. Molony, *Phys. Rev. A* **52**, 1728 (1995).
- [3] M. P. van Exter, M. B. Willemsen, and J. P. Woerdman, *Phys. Rev. A* **58**, 4191 (1998).
- [4] S. Balle, E. Tolkachova, M. San Miguel, J. R. Tredicce, J. Martin-Regalado, and A. Gahl, *Opt. Lett.* **24**, 1121 (1999).
- [5] M. Brambilla, L. A. Lugiato, F. Prati, L. Spinell, and W. J. Firth, *Phys. Rev. Lett.* **79**, 2042 (1997).
- [6] T. Ackeman, S. Barland, M. Cara, S. Balle, J. R. Tredicce, R. Jäger, M. Grabherr, M. Miller, and K. J. Ebeling, *J. Opt. B* **2**, 406 (2000).
- [7] C. Degen, I. Fischer, and W. Elsässer, *Opt. Ex.* **5**, 38 (1999).
- [8] S. P. Hegarty, G. Huyet, J. G. McInerney, and K. D. Choquette, *Phys. Rev. Lett.* **82**, 1434 (1999).
- [9] J. J. Hupert and G. Ott, *Am. J. Phys.* **34**, 260 (1966).
- [10] S. Sridhar, *Phys. Rev. Lett.* **67**, 785 (1991).
- [11] J. Stein and H. J. Stöckmann, *Phys. Rev. Lett.* **68**, 2867 (1992).
- [12] R. Akis, D. K. Ferry, and J. P. Bird, *Phys. Rev. Lett.* **79**, 123 (1997).
- [13] R. Akis, D. K. Ferry, J. P. bird, and D. Vasileska, *Phys. Rev. B* **60**, 2680 (1999).
- [14] Y. H. Kim, M. Barth, H. J. Stöckmann, and J. P. Bird, *Phys. Rev. B* **65**, 165317 (2002).
- [15] D. L. Kaufman, I. Kosztin, and K. Schulten, *Am. J. Phys.* **67**, 133 (1999).
- [16] J. U. Nöckel and A. D. Stone, *Nature (London)* **385**, 45 (1997).
- [17] D. Delande and D. Sornette, *J. Acoust. Soc. Am.* **101**, 1793 (1997).
- [18] A. Bäcker and R. Schubert, *J. Phys. A* **32**, 4795 (1999).